Chapter 10
Ultraviolet Light-Emitting Diodes for Water Disinfection

Marlene A. Lange, Tim Kolbe and Martin Jekel

Abstract This chapter presents basic principles of water disinfection using UV light. It provides a comparison of conventional UV light sources and UV LEDs. Additionally, based on a detailed case study, the potential of UV LEDs for water disinfection systems is discussed. This study presents results of static and flow-through tests conducted with UV LEDs of different emission wavelengths.

10.1 Introduction

In the modern world, more than ever, potable water quality is an issue of global concern, particularly with regard to health care and health protection. This is reflected above all in the fact that 2.2 million people die every year from diarrhea associated with pathogens transmitted by drinking water [52].

As a measure to reduce the risk of infections associated with high levels of microorganisms, water disinfection methods have been developed using physical or chemical disinfection techniques [23].

The original version of this chapter was revised: The spelling of the first author's name was corrected. The erratum to this chapter is available at DOI 10.1007/978-3-319-24100-5_16

M.A. Lange · M. Jekel
Technische Universität Berlin, Fachgebiet Wasserreinhaltung,
Sekr. KF4, Straße des 17 Juni 135, 10623 Berlin, Germany
e-mail: marlange@posteo.de

M. Jekel
e-mail: martin.jekel@tu-berlin.de

T. Kolbe (✉)
Ferdinand-Braun-Institut, Leibniz-Institut für Höchstfrequenztechnik,
Gustav-Kirchhoff-Straße 4, 12489 Berlin, Germany
e-mail: tim.kolbe@fbh-berlin.de

M. Kneissl and J. Rass (eds.), *III-Nitride Ultraviolet Emitters*,
Springer Series in Materials Science 227, DOI 10.1007/978-3-319-24100-5_10

A proven physical disinfection method in drinking water purification is the use of ultraviolet (UV) light with wavelengths between approximately 200–300 nm to inactivate microorganisms [5, 17]. The wavelength of the applied UV light depends on the implemented UV emitter. Conventionally low- and medium-pressure mercury lamps are used; their application for water disinfection of stationary water systems is well investigated (e.g., [3, 27, 32]). More recently, UV light-emitting diodes (LEDs)—for which the emitted wavelength can be adjusted to the target wavelength—are of great interest for water disinfection.

Compared to other techniques, UV disinfection is relatively inexpensive with low capital and operating costs. A UV reactor has a low weight, small footprint and is easy to operate [5]. Owing to these properties, UV disinfection is a promising technique to ensure safe potable water quality. However, UV disinfection is highly dependent on electrical power, since no UV light is produced during power supply interruptions. Moreover, some microorganisms are able to reactivate after UV exposure (cp., e.g., review of [22]). Finally, UV light has no residual disinfection capacity and regrowth may deteriorate water quality after UV disinfection [5].

In water purification applications, particularly in discontinuously operated, decentralized, and mobile water systems, UV LEDs have some advantages compared to conventional UV emitters: LEDs do not contain mercury and the overall system architecture does not need counteractive measures for the breakage of a mercury UV lamp during operation which may contaminate the water, nor is a disposal problem given. LEDs have a compact and robust design without glass or filaments and are therefore more durable in transit and during handling. LEDs have low electrical power requirements and need lower voltages than conventional mercury lamps therefore offering the option to be operated with solar cells or rechargeable batteries. They are more suitable for just-in-time applications because no warm-up time is needed and high frequencies of activation and deactivation are possible without reducing their efficiency [10, 48]. However, at this state of development, UV LEDs suffer from high costs, low output powers, and high initial degradation [32, 53].

10.2 Basic Principles of UV Disinfection

Based on the ability of UV light—produced from conventional or innovative light sources—to function as a broad-spectrum antimicrobial agent with short contact times and minimal disinfection by-product formation, it is a viable alternative to chemical disinfectants. UV light at the proper *wavelength* and *fluence* inactivates microorganisms [20] by disrupting their DNA or RNA, rendering them unable to reproduce.

Wavelength In water purification, wavelengths below 230 nm are absorbed by water molecules. Therefore only UV wavelengths between 230 and 300 nm are available for disinfection. Within this wavelength range, DNA and RNA are the components of microorganisms, which mostly absorb UV light. Proteins, which also absorb UV light, need high fluences at wavelengths below 230 nm (not applied in water disinfection) to be destroyed. Therefore disinfection is mainly achieved by DNA/RNA disruption (e.g., [3, 17, 21, 27]).

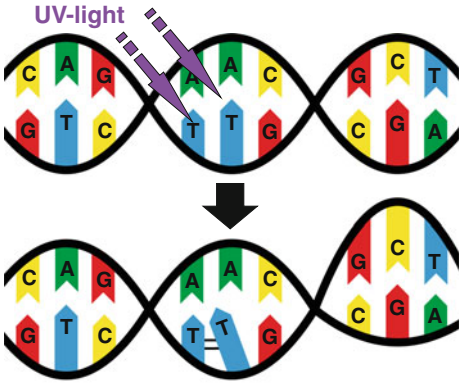

Fig. 10.1 Disruption of DNA structure caused by UV-light-induced thymine dimer formation (*A* adenine, *G* guanine, *T* thymine, *C* cytosine)

DNA and RNA are built up by nucleotides forming polynucleotides. These nucleotides are composed of a backbone made of alternating sugars and phosphate groups; and nucleobases—guanine (G), adenine (A), thymine (T) or uracil in RNA, and cytosine (C)—attached to the sugars. The specific sequence of the DNA/RNA is determined by the order of the nucleobases [31].

UV light is absorbed by all nucleobases. However, UV light may induce dimerization of adjacent thymine/uracil bases causing a chemical bond between these bases (cp. Fig. 10.1). These dimers disrupt the structure of the DNA/RNA and above a critical number of dimers impede the DNA/RNA replication. The microorganism may still be metabolically active, but infections are prevented since reproduction is hindered [5].

Maximum UV light absorption through DNA is typically reached at a wavelength of around 260 nm, but the peak wavelength distribution depends on the target organism [5, 11, 15]. For example *Bacillus subtilis* spores—which are often applied as surrogate organism for protozoan oocysts [22] and in UV reactor certification [17, 38, 47]—have two absorption maxima: one below 240 nm and one around 270 nm [7, 11, 33]. Chen et al. [11] also demonstrated that *B. subtilis* spores have similar fluence–inactivation response curves for 254 and 279 nm wavelengths (cp. Fig. 10.2).[1]

Fluence The term fluence is used in UV disinfection to describe the applied UV "dose". Dose is a term that relates to the total absorbed energy. Since microorganisms only absorb a few percent of the UV light, while the rest of the light passes through the organism, the term *fluence* is more appropriate for UV disinfection than the term dose. Fluence relates to the incident UV energy, rather than the absorbed UV energy [5].

Fluence (J/m^2) is defined as the total amount of radiant energy from all directions passing through an infinitesimally small sphere of cross-sectional area (dA) divided

[1]The same fluence is needed at both wavelengths to obtain a comparable inactivation result.

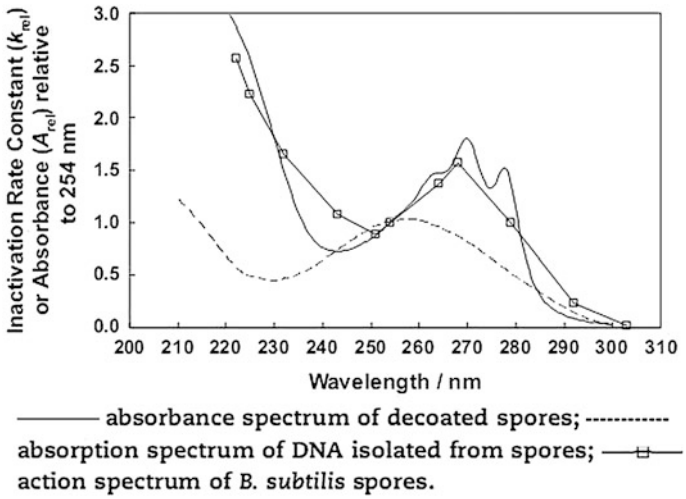

Fig. 10.2 Inactivation rate constant (k) (cp. Sect. 10.3.2.2) of decoated *B. subtilis* spores, DNA isolated from *B. subtilis* spores, and *B. subtilis* spores at different wavelengths [11]

by dA. It is calculated as the product of incident irradiance (or fluence rate) (W/m^2) and exposure time (s) (10.1) [6]:

$$H_0 = E_0 \cdot t \tag{10.1}$$

H_0 fluence (J/m^2)
E_0 incident irradiance (W/m^2)
t exposure time (s).

Irradiance is the appropriate term when a surface is irradiated by UV light coming from all directions above the surface. In a well-designed bench-scale setup—as e.g., a "collimated beam device" (CBD) which delivers a highly uniform beam of UV light to a water sample in a Petri dish—the fluence rate and the irradiance are nearly the same. Fluence rate, instead of irradiance or intensity, is the appropriate term for UV disinfection in a UV reactor, since UV light can penetrate the microorganism from any direction [4]. The fluence rate then is the radiant power passing from all directions through an infinitesimally small sphere of cross-sectional area dA divided by dA (SI unit: W/m^2) [6].

To achieve an optimum disinfection, it is crucial to accurately determine the fluence. Since various factors have been found to have an impact on the applied fluence in UV reactors, it is important to understand these factors (cp. Sect. 10.2.1) and use appropriate modeling and validation tools for UV reactor performance (cp. Sect. 10.2.2), taking these influencing factors into account.

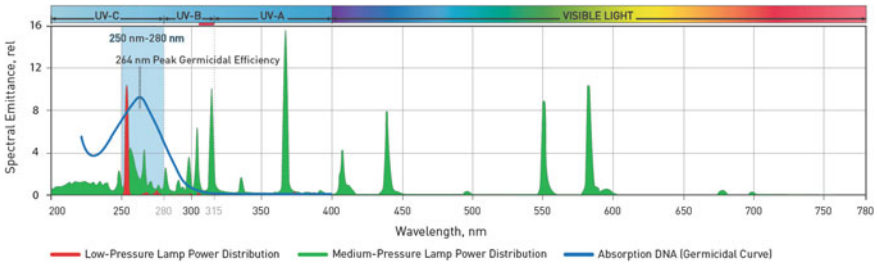

Fig. 10.3 Emission spectra of a typical low-pressure and a medium-pressure UV lamp (Copyrighted work of Pentair Aquatic Eco-Systems, Inc. Used by permission of owner. All rights reserved.)

10.2.1 Factors Influencing UV Fluence

A great deal of research has been undertaken to investigate the factors impacting on UV fluence. Researchers have found that factors like lamp performance, water quality, and exposure time influence the delivered fluence (cp., e.g. [8, 9, 46]).

Lamp Performance Various wavelengths are emitted, depending on the UV light source (cp. Fig. 10.3). Conventionally, UV light is generated from mercury-vapor lamps. Low-pressure (LP) and low-pressure high output (LPHO) lamps emit nearly monochromatic UV light at a wavelength of 254 nm, whereas medium-pressure lamps emit a polychromatic spectrum with various wavelengths [5].

Low-pressure mercury lamps have a higher germicidal efficiency, but lower output powers. They are therefore more suitable for smaller applications. The optimum operation temperature of their lamp bulbs is commonly 40 °C. With increasing or decreasing temperatures, the lamp performance is reduced [5].

Medium-pressure lamps have a lower germicidal efficiency, however, they are installed in applications with high flow rates because they have higher output powers and a smaller number of lamps are needed, thus reducing maintenance costs. They operate at temperatures between 600 to 900 °C and are therefore less sensitive to temperature changes [5].

A relatively new method to generate UV light is by means of LEDs [48]. UV LEDs offer the possibility to apply the optimal disinfection wavelength of targeted microorganisms by manipulating the base materials/composition of the alloy (aluminum gallium nitride, AlGaN), instead of using the 254 nm wavelength emitted by low-pressure mercury lamps [48].

However, at this state of development UV LEDs suffer from low output powers and high initial degradation. Even the best UV LEDs exhibit external quantum efficiencies[2] of around 10 % [42].[3] The reasons for the initial degradation are not

[2]External quantum efficiencies: number of photons emitted into free space per second divided by the number of electrons injected into LED per second.

[3]Typical external quantum efficiencies of LEDs used for lightning applications are in the range of 60–70 % [34].

completely understood but most likely related to high defect densities[4] in the AlGaN materials [26]. Several researchers predict a high physical improvement potential for UV LEDs with regard to the reduction of defect densities and the increase of the output efficiency by increasing the heat extraction [1, 24, 25]. For example, Adivarahan et al. [1] presented an output power of 42 mW for a 4 × 4 LED array lamp (approximately 2.6 mW/LED)[5] emitting at 280 nm.

Since the performance of the UV light source changes over its life time, lamp performance is monitored using a UV sensor. This sensor measures the irradiance at a specific position in the UV reactor. The result of the measurement depends on the UV lamp output, the transmittance of the sensor window, the transmittance of the quartz sleeve, and the transmittance of the water. Besides having a direct impact on the transmittance of UV light, the water quality may also influence the transmittance of the sensor window and quartz sleeve by scaling (or inorganic fouling). Temperature induced scaling is more relevant for conventional mercury lamp UV emitters (due to their higher surface temperatures) than for UV LEDs. However, temperature-independent scaling processes may also affect UV LEDs. The water quality therefore has a significant impact on the disinfection result [6].

Physicochemical Water Quality The presence of dissolved and fine-dispersed water constituents absorbing UV light—measured using the spectral absorption coefficient (a) of the filtered and unfiltered water at the target wavelength (conventionally 254 nm)—reduces the UV light available for microorganism inactivation. It is therefore an important design criterion for UV disinfection. The UV transmittance[6] (UVT) can be calculated from the spectral absorption coefficient [5]:

$$\mathrm{UVT_{cm}} = 100 \times 10^{-a \cdot 0.01\,\mathrm{m}} \tag{10.2}$$

Suspended particles causing turbidity may affect UV disinfection by scattering or absorbing UV light or by shielding microorganisms from UV irradiation. Scattering only redirects UV light and the impact on UV disinfection is minimal, whereas absorption and shielding reduces the UV disinfection efficiency [8, 9, 46].

Scaling deposits on the UV light source reduce the irradiation passing through the scaling layer, reducing the UV light available for microorganism inactivation. Especially iron and manganese and also calcium may scale the quartz sleeve [29, 43, 49]. To restore the transmittance of the sleeve, regular, manual cleaning or cleaning using automatic devices is necessary. It was reported that mechanical cleaning devices were effective in removing scaling deposits [37]. However, it was also reported that mechanical cleaning devices may scratch the surface of the quartz

[4]Defect density: number of local faults originating from the production of semiconductors per surface unit.

[5]For comparison: the 282 nm LEDs applied during this study had an output power of 0.65 mW at 20 mA.

[6]$\mathrm{UVT_{cm}}$ (%): percent transmittance in the medium when the path length is 1 cm and the wavelength is 254 nm; a (1/m): spectral absorption coefficient at a specific wavelength; relates to a 1 m path length.

sleeve, promoting irreversible scaling [39]. Balancing the need for restoring UV transmittance by cleaning and the impact of irreversible scaling may limit the frequency of mechanical cleaning [50]. Since there are no methods available to predict the scaling potential of water [49], pilot testing using the target water was recommended [47, 50].

Exposure Time In contrast to collimated beam devices (CBDs) or chemical disinfection systems, the exposure time of a microorganism in a flow-through UV reactor does not equal the time in which the sample is irradiated. Exposure time has to be derived from the flow rate and hydrodynamics in the UV reactor and can therefore not be monitored directly. Flow rate and hydrodynamics determine the specific path of an organism through the reactor and the time during which the organism is irradiated [3, 15]. On their way through the UV reactor some microorganisms receive more, some less than the average fluence, whereby the microorganisms receiving the lower fluence will determine the performance of the UV reactor [5].

Since the fluence applied on a microorganism in a UV reactor depends on these various factors, fluence calculation has to be carried out with care. The methodology implemented for modeling and validation of the UV reactor performance is described in the following section.

10.2.2 Modeling and Validation of UV Reactor Performance

The complex interplay of factors discussed above, which influence the UV disinfection performance in flow-through reactors, led to the development of a method to calibrate the expected performance of full-scale reactors using collimated beam devices (CBDs). This experimental method called biodosimetry was originally proposed by Qualls and Johnson [40]. It includes the following protocol:

In a first step the test suspension including the test organism is sequentially irradiated in a Petri dish. After every irradiation step, a sample is taken and the number of colony forming units (cfu) of the test organism is determined. By comparison of the number of cfu at the different irradiation steps, an inactivation–response curve is derived. In the second step, the inactivation of the applied test organism is determined in the full-scale UV reactor, varying water quality and flow rate. The determined inactivation rate is assigned according to the fluence obtained on bench-scale. This fluence is called the reduction equivalent fluence (REF). A detailed description of the procedure can be found in [6, 28, 45].

In addition to these extensive biodosimetric tests of UV disinfection reactors the REF can be determined using mathematical models[7] [41]. To calculate the REF with a mathematical model, it is necessary to know the path that a microorganism takes through the reactor and the distribution of the radiation in the UV reactor.

[7]The REF may also be determined using dyed microsphere actinometry cp. e.g., [3].

When the residence time of the organism and the fluence rate is known for every infinitesimally small element of the UV reactor, the fluence can be determined by integration along the path of the microorganism. The path of the microorganism is determined by modeling the momentum and mass transfer in the turbulent current. For the determination of the radiation distribution in the UV reactor varying models are used, which differ in their assumptions and restrictions. An often used calculation approach for UV reactors is the Point Source Summation (PSS) model. More details about turbulence and radiation distribution models are presented by [30].

To investigate UV disinfection on bench-scale for conventional mercury lamps, researchers have made considerable headway in standardizing experimental protocols. There are, for example, standards in Europe and the US that specify protocols for performing microorganism inactivation versus fluence for mercury-lamp-based measurements using, e.g., *B. subtilis* spores [18, 47]. However, a standardized protocol to test UV LEDs has not yet been proposed. An adaptation of the protocol for UV LEDs is needed because of the conventional design, whereby the water sample irradiated from the top down is not applicable to UV LEDs: Top-down methods need high power output sources to compensate for losses (e.g., absorption or scattering) between the UV light source and the water sample which cannot be provided by LEDs. According to Bolton and Linden [6], it is not necessary to completely standardize a bench-scale apparatus, but basic guidelines should be considered when designing a modified apparatus for a specific application. Among other aspects, the design has to ensure that the beam irradiating the water sample is reasonably uniform and the divergence is small enough to ensure accurate sensor readings. The fluence for all microorganisms in the suspension has to be kept equal by carefully controlled stirring without vortex [6].

10.3 Case Study

Over the past few years, various researchers have tested UV LEDs for water disinfection applications (cp., e.g. [2, 12, 14, 35, 36, 48, 51, 53]). These studies investigated LEDs with emission wavelengths between 255 and 405 nm. The experiments were mainly conducted in top-down irradiation geometry irradiating water sample volumes between 190 µl and 100 ml.

Most studies applied UV-sensitive microorganisms as *E. coli* as test organism due to the low output power and high costs of LEDs at this stage of development. In the following case study an experimental setup is presented that allows testing of less sensitive organisms as *B. subtilis* spores which are often used as organism in UV unit certification. Batch and flow-through tests are discussed for two different emission wavelengths of the LED array.

10.3.1 Proposal for an Experimental Setup to Test UV LEDs

Two UV LED disinfection modules were designed by the Institute of Solid State Physics in cooperation with the Chair of Water Quality Control of TU Berlin and constructed by the Ferdinand-Braun-Institut in order to perform biodosimetry trials with AlGaN-based UV LEDs emitting at 269 and 282 nm. LEDs were placed on the base of two different test modules to conduct static and flow-through tests. Module I was designed for static tests only. Module II was designed for static and flow-through tests. Schematic diagrams of the experimental setups are shown in Fig. 10.4 (a) static and (b) flow-through.

For static tests (Fig. 10.4a) a Petri dish with a diameter of 6 cm and a 2 mm thick Suprasil® base was placed on top of the UV LED array. The Suprasil® base allows over 90 % of the deep UV light to be transmitted. Homogeneous irradiation of the entire water volume was furthermore ensured by an electrically driven stirrer, installed at the top of the Petri dish. The output power of the LEDs was measured with a UV-sensitive silicon photodiode, ensuring constant irradiation during all microbiological tests.

For conducting flow-through tests (Fig. 10.4b) the Petri dish was replaced by a flow-through reactor. The flow-through reactor body was made of aluminum to increase UV reflection. 6 mm wide and 5 mm deep water channels were milled into the aluminum and the reactor body was then covered with a 2 mm thick Suprasil® window to enable UV exposure of the water channels. The test water flowed from the feed reservoir through the flow-through reactor and was collected in the catchment tank.

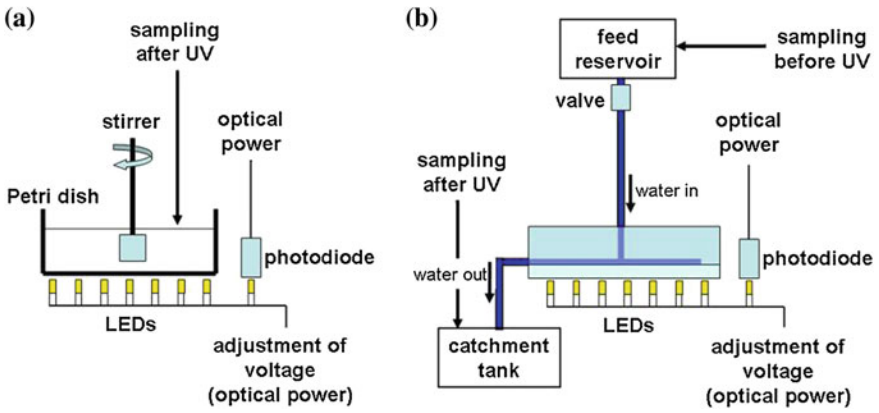

Fig. 10.4 Schematic diagram of the experimental setup for **a** static tests and **b** flow-through tests (according to [53])

The incident irradiance was calculated from (10.3) [6] (UV absorption by the Suprasil® window was neglected):

$$E_0 = \frac{P_{\mathrm{LED}}}{A_{\mathrm{petri}}} \cdot \#_{\mathrm{LED}} \tag{10.3}$$

E_0 incident irradiance (W/m^2)
P_{LED} power output of one LED (W)
A_{petri} area of irradiated Petri dish (m^2)
$\#_{\mathrm{LED}}$ number of active LEDs (–).

Test module I was only designed for static disinfection tests and equipped with 269 nm LEDs. Therefore 33 LEDs were arranged in a hexagonal grid of one LED/cm^2. Owing to the LED array design, only 28.5 of the LEDs were overlapping with the footprint of the Petri dish.

In test module II 35 LEDs with an emission wavelength of 282 nm were positioned in three concentric circles with diameters of 1.8, 3.5, and 5.2 cm. The LEDs were placed on the base of the water disinfection module at a distance of 1 cm in order to obtain a sufficiently high power density and a nearly homogeneous UV light distribution. This test unit was used in the static configuration (Fig. 10.5a) and with the flow-through reactor (Fig. 10.5b) with a maximum flow rate of ~12 ml/min.

A series of the applied UV LEDs was characterized in order to investigate the optimum operating conditions for the water disinfection modules. The module characteristics are summarized in Table 10.1.

LEDs were characterized with respect to their emission spectra, current–voltage and power–current properties, and their development of emission power over time, to select LEDs with similar characteristics.

Spectra were measured under continuous wave (cw) conditions at 20 mA with an optical fiber spectrometer. No variation in the peak wavelength was observed for the different 269 nm LEDs. UV LEDs emitting at 282 nm showed a difference less

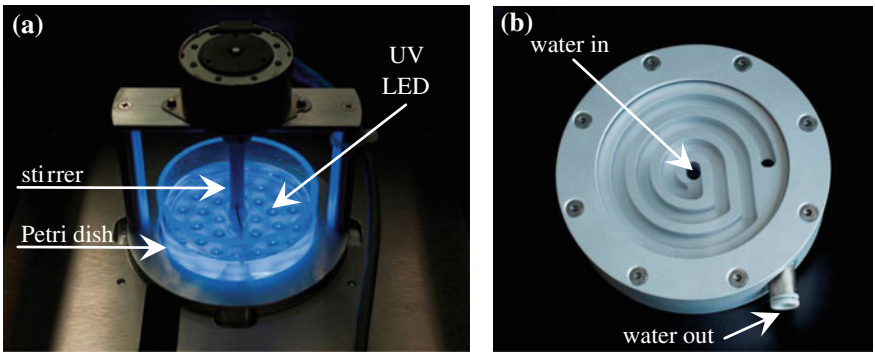

Fig. 10.5 Test module II; **a** LED array with stirrer unit; **b** flow-through reactor (according to [53])

Table 10.1 LED parameters (mean values) during stationary tests of the disinfection modules

Module	LED wavelength (nm)	LED output power (mW)	Number of LEDs	Number of active LEDs	LED configuration	Module output power (mW)
I	269	0.16	33	28.5	1/cm^2 (hexagonal grid)	4.56
II	282	0.19	35	35	3 circles	6.65

Module II was constructed to also perform flow-through tests (according to [53])

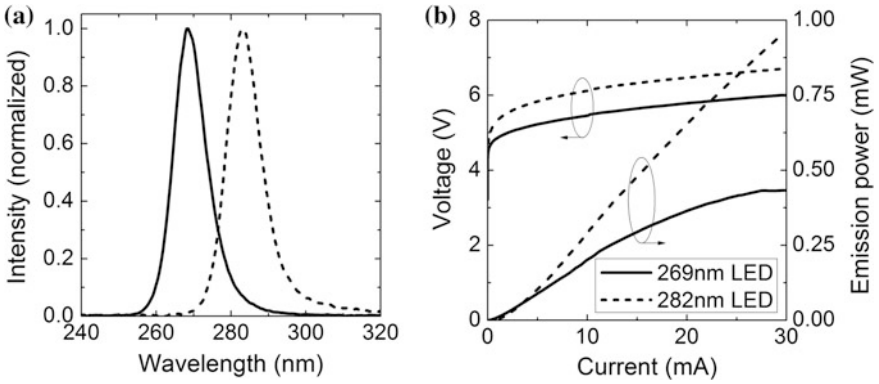

Fig. 10.6 Typical electrical and optical characteristics of 269 and 282 nm LEDs. **a** Emission spectra, **b** current–voltage and current–emission power characteristic

than 1 nm between different LEDs. A typical emission spectrum for both wavelengths is shown in Fig. 10.6a.

The current–voltage characteristics of the UV LEDs were measured at 20 mA under continuous wave (cw) conditions. All LEDs had very similar current–voltage characteristics with typical operating voltages around 5.8 V (269 nm LEDs) and 6.3 V (282 nm LEDs). All LEDs exhibited similar power–current characteristics. The emission power was measured using a calibrated silicon photodiode having a detector area of 100 mm^2. At a current of 20 mA an emission power of 0.33 mW was observed for the 269 nm LEDs and an emission power of 0.65 mW was observed for the 282 nm LEDs (cp. Fig. 10.6b).

The development of emission power over time was monitored for 269 and 282 nm LEDs. In both cases the emission power decreased by around 30–40 % after 100 h of operation at a constant current of 20 mA. The measurement of the current voltage characteristic showed only insignificant differences before and after 100 h of operation time for the 269 and 282 nm LEDs. Additionally, no changes in the emission spectra were observed over time. After the initial drop the emission power nearly stabilized at operating times longer than 100 h. Since maintaining a constant output power is crucial for a water disinfection module, the strong

degradation of the emission power requires active monitoring of the light output during testing and adjustment of the drive current in order to maintain a constant optical power density and fluence.

10.3.2 Test Conditions

10.3.2.1 Disinfection Tests Conducted with UV LEDs

A UV fluence–inactivation response curve of *B. subtilis* ATCC 6633 spores was generated with a laboratory apparatus especially designed for UV LEDs. The test organism was obtained from the Institute of Hygiene and Public Health (University of Bonn, Germany), where it was cultivated and characterized according to the German standard DVGW [18] with monochromatic low-pressure UV lamps [18].

For the exposure tests the applied test organism was suspended in the test water according to DVGW [18] to obtain a concentration of 10^6–10^7 cfu/ml. Tests were conducted at room temperature (23 ± 2 °C). They were performed with stationary samples of 30 ml, and exposed to decreasing fluences.

The fluence was corrected for UV absorbance considering the water factor as presented in (10.4),

$$H_0 = E_0 \cdot \mathrm{WF} \cdot t \tag{10.4}$$

H_0 fluence (J/m^2)
E_0 incident irradiance (W/m^2)
WF water factor (–)
t exposure time (s).

The water factor was derived from integrating the Beer–Lambert Law (10.6) over the sample depth of a completely mixed sample according to [6] as presented in (10.5):

$$\mathrm{WF} = \frac{1 - 10^{-a \cdot d}}{a \cdot d \cdot \ln(10)} \tag{10.5}$$

WF water factor (–)
a spectral absorption coefficient (1/m)
d depths of the suspension (m)
t exposure time (s).

Beer–Lambert Law is

$$a = \log \frac{E_0}{E_t} \tag{10.6}$$

a spectral absorption coefficient (1/m)
E_0 incident irradiance (W/m^2)
E_t transmitted irradiance (W/m^2).

To avoid contamination due to microorganism carryover, disinfection tests were conducted starting with the highest fluence.

During static tests with the 269 nm LEDs, samples of 1.5 ml were taken after 372, 248, 155, 62, and 0 s. Samples of the tests conducted with the 282 nm LEDs were taken after 255, 170, 106, 43, and 0 s to achieve comparable fluences (approx. 600, 400, 250, 100, 0 J/m^2).

Flow-through tests were performed with the 282 nm LEDs in a single pass operation mode. Different fluences were obtained by varying the flow rate and optical output power of the LEDs. Flow rates were chosen based on limitations of the module design and the available light output power from the UV LEDs resulting in laminar conditions. Table 10.2 summarizes the test conditions of the flow-through tests.

The experiments were performed based on DVGW [18] starting with the highest fluence. The following test protocol was applied:

1. initializing the system (adjustment of flow rate and UV power)
2. sampling in reservoir, before UV exposure
3. turning on UV light
4. starting flow, discarding five test cell volumes
5. sampling after UV exposure (after 1, 2, 3, and 4 min)
6. repeated sampling in feed reservoir, before UV exposure.

The concentration of *B. subtilis* spores determined before UV disinfection was calculated by averaging the test results of the samples taken from the reservoir prior to UV exposure.

Table 10.2 Test conditions applied during flow-through tests with 282 nm UV LEDs

Flow rate (ml/min)	Residence time (s)	LED power (mW)
10.8 ± 0.4	45.8	0.50; 0.70
7.8 ± 0.4	63.5	0.35; 0.49

10.3.2.2 Microbial Data Analysis

The inactivation of *B. subtilis* spores, presented as the decimal reduction factor (RF), was calculated based on (10.7)

$$\mathrm{RF} = \log \frac{N_0}{N} \tag{10.7}$$

RF decimal reduction factor
N_0 cfu concentration determined before UV
N cfu concentration determined after UV.

The RF was plotted against fluence to derive a fluence–inactivation relation. The fluence–inactivation response curve of *B. subtilis* spores can be described by three phases [22]: a shoulder phase, a log-linear phase, and a tailing phase. When low fluences are applied the RF changes only slightly with increasing fluence. Researchers attributed this phase to DNA repair or the requirement of several DNA damage sites [33, 44]. After an offset fluence, inactivation starts in a log-linear relationship, followed by an occasionally existing tailing phase, in which the RF again changes slowly with fluence. Causes for the tailing phase are still under discussion; possible causes could be microorganism clumping or association with particles, experimental bias or hydraulic effects [13]. This curve progression, not considering the tailing phase, was described by a shoulder model [22]:

$$\mathrm{RF} = k \cdot \mathrm{Fluence} - b \tag{10.8}$$

RF decimal reduction factor
k inactivation rate constant (m^2/J)
b offset value (crosses the fluence axis at the fluence, where log-linear relation ship starts).

The sensitivity of *B. subtilis* spores was determined from linear regression of the RF between fluences presenting a log-linear relationship. The goodness of fit of the linear regression was analyzed with the coefficient of determination (r^2) and the standard error (StE; the StE measures the error in predicting $f(x) = y$ for an individual x in the regression).

The error of the mean value was calculated according to the following equation [19]:

$$\sigma_{\bar{\mu}} = \pm \frac{\sqrt{\bar{\mu}}}{\sqrt{n}} \tag{10.9}$$

$\sigma_{\bar{\mu}}$ error of the mean value
$\bar{\mu}$ standard deviation
n number of measurements.

Table 10.3 Water quality parameters (mean values) of the applied test waters

	Parameter	Unit	DI	TW	SW	SE
Test waters for tests conducted with 269 nm LEDs						
Unfiltered	a (254)	(1/m)	1.1	–	–	–
	UVT (254)	(%)	97.5	–	–	–
Filtered	a (254)	(1/m)	0.8	–	–	–
	UVT (254)	(%)	98.2	–	–	–
Test waters for tests conducted with 282 nm LEDs						
Unfiltered	a (254)	(1/m)	2.7	10.8	18.4	28.7
	UVT (254)	(%)	94.1	78.0	65.5	51.7
	a (282)	(1/m)	2.3	8.2	13.4	22.1
	UVT (282)	(%)	94.8	82.8	73.5	60.1
Filtered	a (254)	(1/m)	0.7	7.9	15.9	23.6
	UVT (254)	(%)	98.4	83.4	69.3	58.1
	a (282)	(1/m)	0.4	5.4	11.0	17.6
	UVT (282)	(%)	99.0	88.3	77.6	66.7

DI deionized water, *TW* tap water, *SW* surface water, *SE* secondary effluent

10.3.2.3 Physicochemical Water Quality

Tests were performed with different water qualities: deionized water (DI), tap water (TW), surface water (SW), and secondary effluent (SE). Water samples were taken in Berlin, Germany. Tap water was obtained from the local water supply of the city of Berlin. Surface water samples were taken at the Landwehrkanal and secondary effluent was provided by the waste water treatment plant Ruhleben.[8]

Table 10.3 summarizes the measured and calculated water absorption parameters for wavelength of a conventional low-pressure mercury lamp (254 nm) and a UV LED with an emission of 282 nm. The UV absorption (a) was measured with a two beam spectrometer in a 5 cm quartz cuvette. Afterwards the UV transmittance (UVT) was calculated from (10.2).

The high turbidity of the *B. subtilis* suspension reduced UVT (254) of the unfiltered deionized water samples. Higher absorption of the test waters used in experiments with the 282 nm LEDs was caused by a higher initial spore concentration. The tap water of the city of Berlin contains a high amount of UV active dissolved organic matter, resulting in a high UV absorbance of the tap water test samples.

[8]The waste water treatment plant Ruhleben treats combined municipal waste water with parts of rainwater by mechanical separation, activated sludge process with nitrification, post-denitrification, and biological phosphorus removal.

10.3.3 Results of Tests Conducted with UV LEDs

The potential of UV LEDs for mobile water disinfection was investigated in three steps: First, a UV LED module was constructed, tested with various water qualities, and the results were compared to results obtained with a conventional standardized mercury lamp system (cp. Sect. 10.3.3.1). Then, the influence of two different LED wavelengths on the disinfection of *B. subtilis* spores was compared based on their disinfection capacity and power consumption (cp. Sect. 10.3.3.2). Finally, real water disinfection applications were simulated with a bench-scale flow-through reactor (cp. Sect. 10.3.3.3).

10.3.3.1 Module Development and Validation

The test modules were developed based on the low output power of the UV LEDs causing long irradiation times and low flow rates. The design consisted of a LED array, irradiating the water sample from the bottom up, in contrast to the conventional collimated beam device (CBD), in which the mercury lamp is located on top of the water sample. The inhomogeneous light emission was addressed by constant stirring during static tests. Validation tests were performed with arrays of UV LEDs emitting at 282 nm. *B. subtilis* spores were used as test organism and exposed successively to UV light.

In the first step of the validation process, the reproducibility of test results obtained with the designed module was evaluated by the error of mean value of repeated tests and by applying various water qualities. In the second step of the validation, test results were compared to disinfection tests conducted on a standardized mercury lamp CBD.

The inactivation results to evaluate the reproducibility of the test module with different water qualities are presented in Fig. 10.7. Increasing UVT was considered in fluence calculation causing lower applied fluences at the same exposure time for waters containing higher amounts of UV absorbing compounds (cp. Equation 10.4).

Linear regression was performed for all data points between 97 and 581 J/m^2 with a high goodness of fit (StE = 0.44; r^2 = 0.94). Data points beneath 97 J/m^2 were not included for data analysis due to a non-log-linear relationship (shoulder effect; cp. Sect. 10.3.2.2).

The maximum error of mean value of the RF in DI water tests was the same as the maximum error of mean value of the triplicate analysis (both 1.5; n = 3). This comparison indicates that the test setup generates reproducible results which are in the range of the triplicate analysis. Reproducibility of the tests conducted with the UV LED test module was also underlined by a highest error of mean value of 0.9 (n = 9) between all conducted experiments.

In a second validation step, *B. subtilis* spores were used under different experimental conditions: in the 282 nm LED module and in a 254 nm mercury lamp

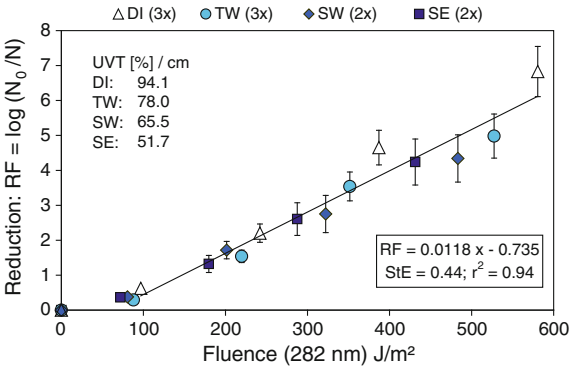

Fig. 10.7 Fluence–inactivation response and curve derived by linear regression of *B. subtilis* spores in different waters (*DI* deionized water, *TW* tap water, *SW* surface water, *SE* secondary effluent) with different qualities (UVT_{254} as representative parameter) for 282 nm LEDs; in parentheses are the numbers of test batches. Presented data are geometric mean values ± error of mean value of three test rows. Test rows were cultivated in triplicates

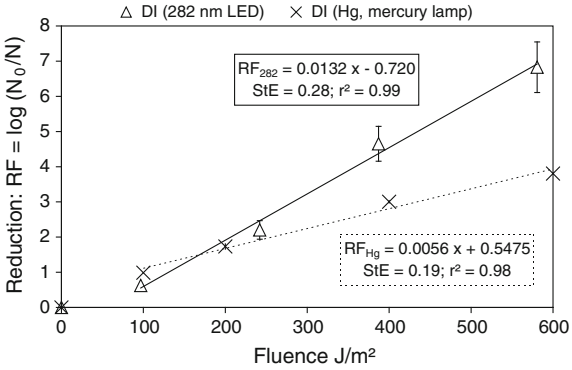

Fig. 10.8 Fluence–inactivation response and curves derived by linear regression of *B. subtilis* spores irradiated with UV light in deionized water for 282 nm LEDs and a mercury lamp. Presented data are geometric mean values ± error of mean value of three test rows. Test rows were cultivated in triplicates

CBD.[9] According to literature data, the fluence–inactivation response curve of *B. subtilis* spores should be comparable at wavelengths of 254 and 279 nm (Fig. 10.2, [11]), and therefore the sensitivity of the surrogate spores should be comparable in both experimental setups.

[9]These CBD tests conducted with a mercury lamp was performed by an external laboratory (Institute of Hygiene and Public Health, University of Bonn).

The UV sensitivity of a microorganism is described by the inactivation rate constant k (m^2/J) and the offset value—b (cp. Sect. 10.3.2.2) derived from linear regression of the reduction factor (RF) over fluence plot. Spore inactivation results in DI water obtained with 282 nm LEDs and a conventional mercury lamp are presented in Fig. 10.8.

Linear regression was performed for fluences above 100 J/m^2, due to a missing log-linear relation ship (offset value). For the 282 nm LEDs a shoulder effect at low fluences was observed (negative offset value). Tailing was neither observed for the 282 nm LEDs nor for the mercury lamp at the investigated fluences. A linear fluence–inactivation relationship was observed in both experimental setups between 100 and 600 J/m^2. Regression analysis led to low StE and r^2 values for the 282 nm LEDs (StE = 0.28, r^2 = 0.99) and the mercury lamp (StE 0.19, r^2 = 0.98).

A comparison of the inactivation rate constants k of the 282 nm LEDs (0.0132 J/m^2) and the mercury lamp (0.0056 J/m^2) indicated a two times higher sensitivity of the *B. subtilis* spores in the LED module. The difference of spore reduction between the 282 nm LEDs and the mercury lamp therefore increased with higher fluences. Based on the assumption that the different wavelengths should result in the same sensitivity (according to [11]), the difference of the disinfection kinetics may have to be attributed to the different experimental setups. Various factors, such as the condition of the test suspension, the fluence calculation, and/or the different constructions of the LED apparatus and the CBD, might have influenced the test results. At this stage, a clear explanation for this higher disinfection capacity at higher fluences compared to the conventional UV source needs further investigation.

However, as the LED system generated reproducible results, the inactivation results obtained for different wavelengths on the same experimental setup are comparable. The influence of different UV LED wavelengths on the disinfection of *B. subtilis* spores is discussed in the following section.

10.3.3.2 Comparison of LEDs Emitting at 282 nm and 269 nm

The disinfection capacity of 269 and 282 nm emitting LEDs was investigated by running disinfection tests with deionized water. According to previous research, the 269 nm wavelength corresponds to the absorption maximum of the *B. subtilis* spores [7, 11, 33] and should therefore show a greater inactivation than the 282 nm LEDs. On the other hand, the 282 nm LEDs have a higher optical power output. The consequences are discussed in the following. Figure 10.9 presents the inactivation curves derived from the results obtained with different UV LED wavelengths in the static apparatus configuration.

Deduced from linear regression, *B. subtilis* was equally sensitive to both wavelengths above 100 J/m^2 (k_{282} = 0.0132; k_{269} = 0.0133). The offset value for the 282 nm LEDs was negative, indicating a shoulder effect, as discussed above. The offset value for the 269 nm LEDs was positive and therefore no shoulder effect existed. As the 269 nm LEDs showed no shoulder effect, the absolute difference of

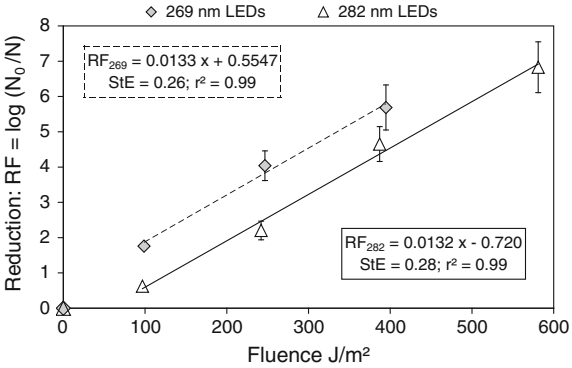

Fig. 10.9 Comparison of fluence–inactivation response and curves derived by linear regression for *B. subtilis* spores in deionized water, obtained with UV LEDs of 269 and 282 nm in the static apparatus. Presented data are geometric mean values ± error of mean value

more than one log in the investigated fluence range demonstrated a higher absolute disinfection using 269 nm LEDs. This enhanced disinfection capacity could be attributed to the higher germicidal efficiency at a wavelength of 269 nm.

In a next step, the 269 and 282 nm LEDs were compared, based on a model calculation considering the same input power and time, which resulted in different fluence. A model calculation was conducted, based on a nominal drive current of 20 mA, at which the 269 nm LEDs have an optical power output of 0.33 mW, whereas the 282 nm LEDs have an optical power output of 0.65 mW. Various resulting fluences were calculated according to (10.3). The resulting inactivation was calculated from the inactivation curves derived in Fig. 10.9. The results of the model calculation are summarized in Table 10.4.

Although the 269 nm LEDs exhibit a higher germicidal efficiency, the spore inactivation caused by the 282 nm LEDs is higher than for the 269 nm LEDs during the same time span and at the same input power. Irradiation for a period of 300 s,

Table 10.4 Summary of model calculation for the comparison of power consumption and inactivation performance of the 269 and 282 nm LEDs; boundary conditions: input current of 20 mA and a total of five LEDs

	269 nm Output: 0.33 mW		282 nm Output: 0.65 mW		Difference
Time (s)	Fluence (J/m^2)	RF_{269} (log N_0/N)	Fluence (J/m^2)	RF_{282} (log N_0/N)	$RF_{282} - RF_{269}$ (log N_0/N)
200	117	1.9	230	2.4	0.5
250	146	2.3	287	3.0	0.7
300	175	2.7	345	3.7	1.0
350	204	3.1	402	4.4	1.3
400	233	3.6	460	5.1	1.5

Reduction factor: $RF_{269} = 0.01133\ x + 0.5547$; $RF_{282} = 0.0132\ x - 0.720$

for example, led to an applied fluence of 175 J/m^2 for the 269 nm LEDs and an applied fluence of 345 J/m^2 for the 282 nm LEDs. At this fluence value the reduction factor for the 269 nm LEDs is 1.0 log lower than for the 282 nm LEDs. This is due to the higher output power (at the same current) of the 282 nm LEDs. The higher disinfection capacity of the 269 nm LEDs, which is due to an output wavelength close to the absorption maximum (around 270 nm) of the *B. subtilis* spores, is compensated by a higher output power of the 282 nm LEDs. As a consequence, the use of 282 nm LEDs is preferable for the overall performance of the UV purification module, as long as the performance of the LEDs at the shorter wavelength is not improved. In the future, with increasing output power of the LEDs available for both wavelengths, the trend may be different. The optimum wavelength will have to be chosen based on a comparison between the UV output power and the reduction factor applying the same fluence.

10.3.3.3 Flow-Through Tests

During this study flow-through tests were conducted with the higher output power 282 nm LEDs. Flow-through tests were performed with a flow-through reactor to obtain first results for the applicability of UV LEDs under real conditions. Differing fluences were obtained by varying the flow rate and optical power output of the 282 nm LEDs (cp. Sect. 10.3.2). The flow rate was adjusted to (10.8 ± 0.4) ml/min and (7.8 ± 0.4) ml/min, resulting in laminar conditions. The results are presented in Fig. 10.10.

Linear regression was performed, including all data obtained with a flow rate of (10.8 ± 0.4) ml/min and (7.8 ± 0.4) ml/min, to investigate whether the flow rates have an influence on the spore inactivation. The low StE of 0.20 and a goodness of

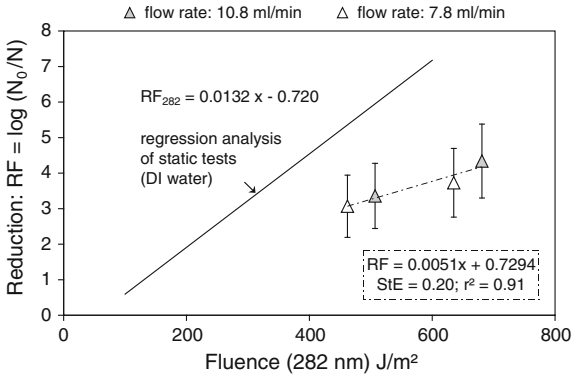

Fig. 10.10 Fluence–inactivation response and the curves derived by linear regression of *B. subtilis* spores in deionized (DI) water, obtained with the apparatus designed for 282 nm UV LEDs in static tests (regression analysis of static tests in DI water) compared to results obtained during flow-through tests. Presented data are geometric mean values ± error of mean value

fit of $r^2 = 0.91$ indicated that—applying laminar conditions—the flow rate has no significant influence on the spore reduction. Therefore, the fluence–inactivation response curve—including data of differing flow rates—was used for further evaluation. With regard to this curve, the sensitivity (inactivation rate constant k) of the *B. subtilis* spores was more than halved in flow-through tests compared to static test results (represented in Fig. 10.10 as regression analysis of static tests). Although nominally the same fluence was applied, the inactivation of *B. subtilis* in the flow-through test reactor was reduced compared to static tests. This is a common phenomenon when scaling up UV reactors and constructing flow-through reactors instead of static reactors. These results indicate that the flow conditions lead to areas of lower UV irradiation by incomplete illumination and short-circuiting by shadowing effects within the flow-through test reactor, reducing the overall disinfection efficiency. Nevertheless, an increase in the applied fluence leads to a higher inactivation, indicating a promising design of the UV LED configuration in the flow-through reactor.

In the German procedure of UV reactor certification for potable water production, a target fluence of 400 J/m^2 is set [16]. Based on the sensitivity of the applied test organism in CBD tests, 400 J/m^2 are achieved when the spores are reduced by three log (cp. Sect. 10.3.2). However, even with a lower sensitivity of the applied test spores in flow-through tests a 3-log reduction in *B. subtilis* spore count was demonstrated, applying only a minimally higher fluence of approx. 450 J/m^2 than needed in CBD tests.

10.4 Potential of UV LEDs for Water Disinfection

The objective of this chapter was to evaluate the suitability of AlGaN-based UV LEDs for water disinfection. Therefore published investigations using UV LEDs were reviewed and results of a case study were summarized.

The case study included the evaluation of the performance characteristics of UV LEDs at different operating conditions as well as the design and development of a UV LED module in view of the requirements for water treatment applications. Bioanalytical testing was conducted using *B. subtilis* spores as test organism and UV LEDs with emission wavelengths of 269 and 282 nm.

Test results indicated an effective inactivation of *B. subtilis* spores through UV LEDs at emitting wavelengths of 269 and 282 nm and therefore a basic applicability of UV LEDs for water disinfection. The higher disinfection efficiency of the 269 nm LEDs than the 282 nm LEDs was compensated by the higher optical output power of the 282 nm LEDs.

In general, the optical output power of the UV LEDs is still very low and needs further improvement in order to make them suitable for real-world applications. Water purification applications where water has to be disinfected within a few seconds are still limited by long exposure times when using UV LEDs. As a consequence, the reactor design would have to be reduced to small diameters.

UV LEDs might therefore only be applicable at the tap outlet, where water flows are lower. On the one hand, this UV disinfection system design would reduce the impact of microbial regrowth in the piping system on the extracted water and increase water quality at the point of use. On the other hand, the installation of various UV light point sources requires the development of a completely new monitoring system. Special attention would have to be paid to UV light emission monitoring for each single UV LED to avoid unperceived UV LED failure and loss of disinfection efficiency.

However, due to the big advantages of UV LEDs—like the tunable emission wavelength, the low voltages, the immediate availability of UV radiation, their robust and compact design, and predicted longer life times—UV LEDs will be promising candidates to realize new disinfection applications in the area of mobile disinfection systems. Additionally, they will be also good candidates for replacing conventional UV disinfection systems especially for applications where only low flow rates are needed. This process will be supported in the future by the continuously increasing development in the UV LED area and the expected reduction of the LED costs through production scale-up due to the increasing demand for such devices.

Acknowledgments The authors thank Boris Lesjean and Eric Hoa from the Berlin Centre of Competence for Water and Florencio Martin from Veolia Water, Anjou Recherche, for their helpful expertise, Katharina Kutz for her laboratory work and the Berliner Wasserbetriebe for providing the samples of secondary effluents. This work was partially supported by the Berlin Centre of Competence for Water in the frame of the FP6 project TECHNEAU, and financed by the European Commission and Veolia Water.

References

1. V. Adivarahan, A. Heidari, B. Zhang, Q. Fareed, S. Hwang, M. Islam, A. Khan, 280 nm deep ultraviolet light emitting diode lamp with an AlGaN multiple quantum well active region. Appl. Phys. Exp. **2**(102101) (2009)
2. J. Bak, S.D. Ladefoged, M. Tvede, T. begovic, A. Gregersen, Disinfection of Pseudomonas aeruginosa biofilm contaminated tube lumens with ultraviolet C light emitting diodes. Biofouling **26**(1), 31–38 (2010)
3. E.R. Blatchley, C. Shen, O.K. Scheible, J.P. Robinson, K. Ragheb, D.E. Bergstrom, D. Rokjer, Validation of large-scale, monochromatic UV disinfection systems for drinking water using dyed microspheres. Water Res. **42**(3), 677–688 (2008)
4. J.R. Bolton, Calculation of ultraviolet fluence rate distributions in an annular reactor: Significance of refraction and reflection. Water Res. **34**(13), 3315–3324 (2000)
5. J.R. Bolton, C.A. Cotton, *The Ultraviolet Disinfection Handbook* (American Water Works Association, Denver, 2008)
6. J.R. Bolton, K.G. Linden, Standardization of methods for fluence (UV dose) determination in bench-scale UV experiments. J. Environ. Eng. ASCE **129**(3), 209–215 (2003)
7. A. Cabaj, R. Sommer, W. Pribil, T. Haider, The spectral UV sensitivity of microorganisms used in biodosimetry. Water Suppl. IWA Publ. **2**(3), 175–181 (2002)

8. R.E. Cantwell, R. Hofmann, Inactivation of indigenous coliform bacteria in unfiltered surface water by ultraviolet light. Water Res. **42**(10–11), 2729–2735 (2008)
9. E. Caron, G. Chevrefils, B. Barbeau, P. Payment, M. Prévost, Impact of microparticles on UV disinfection of indigenous aerobic spores. Water Res. **41**, 4546–4556 (2007)
10. C. Chatterley, K. Linden, Demonstration and evaluation of germicidal UV-LEDs for point-of-use water disinfection. J. Water Health IWA Publ. **8**(3), 479–486 (2010)
11. R.Z. Chen, S.A. Craik, J.R. Bolton, Comparison of the action spectra and relative DNA absorbance spectra of microorganisms: Information important for the determination of germicidal fluence (UV dose) in an ultraviolet disinfection of water. Water Res. **43**(20), 5087–5096 (2009)
12. A.C. Chevremont, A.M. Farnet, M. Sergent, B. Coulomb, J.L. Boudenne, Multivariate optimization of fecal bioindicator inactivation by coupling UV-A and UV-C LEDs. Desalination **285**, 219–225 (2012)
13. S.A. Craik, G.R. Finch, J.R. Bolton, M. Belosevic, Inactivation of Giardia muris cysts using medium-pressure ultraviolet radiation in filtered drinking water. Water Res. **34**(18), 4325–4332 (2000)
14. M.H. Crawford, M.A. Banas, M.P. Ross, D.S. Ruby, J.S. Nelson, R. Boucher, A.A. Allerman, *Final LDRD Report: Ultraviolet Water Purification Systems for Rural Environments and Mobile Applications* (Sandria National Laboratories, Albuquerque, New Mexico, 2005), pp. 1–37
15. J.C. Crittenden, R.R. Trussell, D.W. Hand, K.J. Howe, G. Tchobanoglous, Disinfection with ultraviolet light, in *Water Treatment: Principles and Design*, Chapter 13.8 (Wiley, Hoboken, 2005)
16. DVGW, *Arbeitsblatt W 290: Trinkwasserdesinfektion - Einsatz und Anforderungskriterien* (Deutsche Vereinigung des Gas- und Wasserfaches, Bonn, 2005)
17. DVGW, *Arbeitsblatt W 294-1: UV-Geräte zur Desinfektion in der Wasserversorgung Teil 1: Anforderungen an Beschaffenheit, Funktion und Betrieb* (Deutsche Vereinigung des Gas- und Wasserfaches, Bonn, 2006a)
18. DVGW, *Arbeitsblatt W 294-2: UV-Geräte zur Desinfektion in der Wasserversorgung Teil 2: Prüfung von Beschaffenheit, Funktion und Desinfektionswirkung* (Deutsche Vereinigung des Gas- und Wasserfaches, Bonn, 2006b)
19. F. Embacher, *Mathematische Grundlagen für das Lehramtsstudium Physik* (Vieweg + Teubner | GWV Fachverlage GmbH, Wiesbaden, 2011)
20. F.L. Gates, A study of the bactericidal action of ultraviolet light: III. The absorption of ultraviolet light by bacteria. J. Gen. Physiol. **14**(1), 31–42 (1930)
21. W. Harm, *Biological Effects of Ultraviolet Radiation* (Cambridge University Press, New York, 1980)
22. W.A.M. Hijnen, E.F. Beerendonk, G.J. Medema, Inactivation credit of UV radiation for viruses, bacteria and protozoan (oo)cysts in water: A review. Water Res. **40**(1), 3–22 (2006)
23. K. Höll, *Wasser. Nutzung im Kreislauf. Hygiene, Analyse und Bewertung.* (Walter de Gruyter, Berlin, 2002)
24. A. Khan, K. Balakrishnan, T. Katona, Ultraviolet light-emitting diodes based on group three nitrides. Nat. Photon. **2**, 77–84 (2008)
25. M. Kneissl, Ultraviolet light-emitting diodes promise new solutions for water purification. World Water & Environmental Engineering **31**(3), 35 (2008)
26. T. Kolbe, *Einfluss des Heterostrukturdesigns auf die Effzienz und die optische Polarisation von (In)AlGaN-basierten Leuchtdioden im ultravioletten Spektralbereich*. Ph.D. Thesis, Fakultät II - Mathematik und Naturwissenschaften; Technische Universität Berlin, Berlin, 2012
27. A. Kolch, UV-Disinfection of drinking water—the new DVGW work sheet 94 Part 1–3. IUVA News **9**, 17–20 (2007)

28. J. Kuo, C.L. Chen, M. Nellor, Standardized collimated beam testing protocol for water/wastewater ultraviolet disinfection. J. Environ. Eng. ASCE **129**(8), 774–779 (2003)
29. L.-S. Lin, C.T. Johnston, E.R. Blatchley III, Inorganic fouling at quartz: Water interfaces in ultraviolet photoreactors: II. Temporal and spatial distributions. Water Res. **33**(15), 3330–3338 (1999)
30. D. Liu, *Numerical Simulation of UV Disinfection Reactors: Impact of Fluence Rate Distribution and Turbulence Modeling*. Dissertation, North Carolina State University, 2004
31. M.T. Madigan, J.M. Martinko, J. Parker, *Makromoleküle*. In: *Brock Mikrobiologie*, Chapter 24 (W. Goebel. Spektrum Akademischer Verlag GmbH, Heidelberg, 2001)
32. J.P. Malley, UV in water treatment issues for the next decade. IUVA News **12**(1), 18–25 (2010)
33. H. Mamane-Gravetz, K.G. Linden, A. Cabaj, R. Sommer, Spectral sensitivity of Bacillus subtilis spores and MS2 Coliphage for validation testing of ultraviolet reactors for water disinfection. Environ. Sci. Technol. **39**(20), 7845–7852 (2005)
34. T. Miyoshi, T. Yanamoto, T. Kozaki, S.-I. Nagahama, Y. Narukawa, M. Sano, T. Yamada, T. Mukai, *Recent status of white LEDs and nitride LDs* (2008)
35. K.Y. Nelson, D.W. McMartin, C.K. Yost, K.J. Runtz, T. Ono, Point-of-use water disinfection using UV light-emitting diodes to reduce bacterial contamination. Environ. Sci. Pollut. Res. **20**(8), 5441–5448 (2013)
36. K. Oguma, R. Kita, H. Sakai, M. Murakami, S. Takizawa, Application of UV light emitting diodes to batch and flow-through water disinfection systems. Desalination **328**, 24–30 (2013)
37. M. Oliver, UV cleaning system performance validation. IUVA News **5**(1)
38. ÖNORM, *Plants for Disinfection of Water Using Ultraviolet Radiation: Requirements and Testing, Part 1: Low Pressure Mercury Lamp Plants* (Austrian Standards Institute, Vienna, 2001), www.on-norm.at
39. J. Peng, Y. Qiu, R. Gehr, Characterization of permanent fouling on the surfaces of UV lamps used for wastewater disinfection. Water Environ. Res. **77**(4), 309–322 (2005)
40. R.G. Qualls, J.D. Johnson, Bioassay and dose measurement in UV disinfection. Appl. Environ. Microbiol. **45**(3), 872–877 (1983)
41. C. Reichl, C. Buchner, G. Hirschmann, R. Sommer, A. Cabaj, *Development of a Simulation Method to Predict UV Disinfection Reactor Performance and Comparison to Biodosimetric Measurements*. *Conference on Modelling Fluid Flow*, Budapest (2006)
42. M. Shatalov, W. Sun, A. Lunev, X. Hu, A. Dobrinsky, Y. Bilenko, J. Yang, M. Shur, R. Gaska, C. Moe, G. Garrett, M. Wraback, AlGaN deep-ultraviolet light-emitting diodes with external quantum efficiency above 10 %. Appl. Phys. Exp. **5**(8), 082101 1–3 (2012)
43. M. Sheriff, R. Gehr, Laboratory investigation of inorganic fouling of low pressure UV disinfection lamps. Water Qual. Res. J. Can. **36**(1), 71–92 (2001)
44. R. Sommer, A. Cabaj, T. Sandu, M. Lhotsky, Measurement of UV radiation using suspensions of microorganisms. J. Photochem. Photobiol. B **53**(1–3), 1–6 (1999)
45. R. Sommer, A. Cabaj, D. Schoenen, J. Gebel, A. Kolch, A.H. Havelaar, F.M. Schets, Comparison of three laboratory devices for UV-inactivation of microorganisms. Water Sci. Technol. **31**(5–6), 147–156 (1995)
46. M.R. Templeton, R.C. Andrews, R. Hofmann, Inactivation of particle-associated viral surrogates by ultraviolet light. Water Res. **39**, 3487–3500 (2005)
47. USEPA, *Ultraviolet Disinfection Guidance Manual for the Final Long Term 2 Enhanced Surface Water Treatment Rule. 815-R-06-007,* Washington DC (2006)
48. S. Vilhunen, H. Särkkä, M. Sillanpää, Ultraviolet light-emitting diodes in water disinfection. Environ. Sci. Pollut. Res. **16**(4), 439–442 (2009)
49. I.W. Wait, C.T. Johnston, E.R. Blatchley III, The influence of oxidation reduction potential and water treatment processes on quartz lamp sleeve fouling in ultraviolet disinfection reactors. Water Res. **41**(11), 2427–2436 (2007)

50. I.W. Wait, M. Yonkin, E.R. Blatchley III, *Quartz lamp sleeve fouling and cleaning system evaluation at the Albany, New York Loudonville UV treatment facility*. IUVA News **8**(4), 11–14 (2006)
51. S. Wengraitis, P. McCubbin, M.M. Wade, T.D. Biggs, S. Hall, L.I. Williams, A.W. Zulich, *Pulsed UV-C disinfection of Escherichia coli with light-emitting diodes, emitted at various repetition rates and duty cycles*. Photochem. Photobiol. **89**, 127–131 (2013)
52. WHO, *Water for Health—WHO Guidelines for Drinking-water Quality* (WHO Press, 2010)
53. M.A. Würtele, T. Kolbe, M. Lipsz, A. Külberg, M. Weyers, M. Kneissl, M. Jekel, Application of GaN-based ultraviolet-C light emitting diodes—UV LEDs—for water disinfection. Water Res. **45**(3), 1481–1489 (2011)